

## 1/F NOISE OF INDIUM NEAR THE MELTING TRANSITION

John H. Scofield\* , R. W. Epworth and D. M. Tennant  
AT&T Bell Laboratories, Holmdel, NJ 07733

Measurements of the resistance and 1/f noise of continuous thin film indium conductors in the temperature range 140 °C to 160 °C for frequencies 0.1 Hz to 256 Hz are reported. The 250 nm thick, 500 nm wide, 5.0 mm long, six-probe conductors were fabricated on an oxidized silicon wafer using e-beam lithography, and were encapsulated with a 500 nm thick layer of Si<sub>3</sub>Ni<sub>4</sub>. Upon heating, melting occurred at (156 ± 1) °C, whereas upon cooling, solidification occurred at (152 ± 1) °C. The band-limited variance  $\langle \delta r^2 \rangle$  of the resistance fluctuations was a factor of 10 lower for the liquid than for the solid, while the resistance of the liquid was nearly twice that of the solid. Hence, the relative 1/f noise of the liquid was nearly 40 times lower than that of the solid, in conflict with the results of two-probe measurements on liquid gallium found in the literature. These new results are consistent with models that attribute the 1/f noise of metals to defects and inconsistent with models that relate the noise to intrinsic mechanisms like phonon scattering or infrared divergences.

**Revision Date:** April 20, 1989

**PACS:** 72.70+M, 73.60+Dt, 05.40+j, 61.25+Mv

### I. Introduction

Much evidence now suggests that 1/f noise is not intrinsic to metallic conduction, but rather, is associated with defects in the thin films used to study the phenomenon [1-5]. The noise is thought to be caused by changes in scattering due to the slow relaxation and/or rearrangement of defects [6-8]. While there is some evidence implicating grain boundaries in aluminum films [5] and point defects in Cu films [4] the importance of various defects in generating 1/f noise remains an open question. In particular, it is not yet clear whether impurities or structural defects are more important in producing 1/f noise.

It has been reported that liquid and solid gallium point contacts have similar 1/f noise [9] suggesting that crystalline structure, or lack thereof (i.e., lattice defects) does not play an important role in producing 1/f noise. Moreover, due to the rapid diffusion of defects in a liquid metal, it is doubtful that any defect mechanism would yield sufficiently long time scales to give 1/f noise. Two-probe measurements, however, may be sensitive to surface effects, and thus yield incorrect results [10].

In this paper we report the results of four-probe measurements of the noise of a liquid metal. These samples are believed to be the smallest liquid metal structures to be used with transport measurements, and the first reliable measurements of the 1/f noise of a liquid metal. Indium, rather than gallium, was chosen so that sample fabrication could be accomplished using standard lithography techniques. In contrast to the two-probe gallium result we find that the 1/f noise of these indium samples decreases by an order of magnitude upon

melting. These results are consistent with several defect models for 1/f noise.

### II. Experiment

The sample fabrication process is briefly summarized below; a detailed description has been given elsewhere [11]. Samples were fabricated as tri-level structures on an insulating substrate (see Figure 1(a)). A 200 nm thick layer of tungsten was deposited onto an oxidized silicon wafer and subtractively patterned (with photolithography followed by ion-milling) to form contact leads on 6 mm x 6 mm chips. Next, the entire wafer was coated with polymethylmethacrylate (PMMA), and high-resolution, wafer-scale e-beam lithography used to write liftoff patterns for large leads connecting to submicron multi-probe conductors. (The lead portion of the e-beam pattern provided a region of overlap onto the previously patterned tungsten leads on each chip.) The wafer was cleaved into individual chips for subsequent processing. Indium was thermally evaporated onto chips cooled to liquid nitrogen temperature and subsequently lifted off in acetone. Smooth indium films with good adhesion were achieved using the method described by Chiao et.al. [12]. Figure 1(b) is a scanning electron micrograph of the conductor region of an indium sample made using this technique. All samples discussed here have lengths  $L = (5.0 \pm 0.3) \mu\text{m}$  and widths  $w = (600 \pm 100) \text{nm}$ ; thicknesses  $t$  varied from sample to sample, ranging between 100 nm and 250 nm.

\* Present address: Physics Department, Oberlin College, Oberlin, OH 44074.

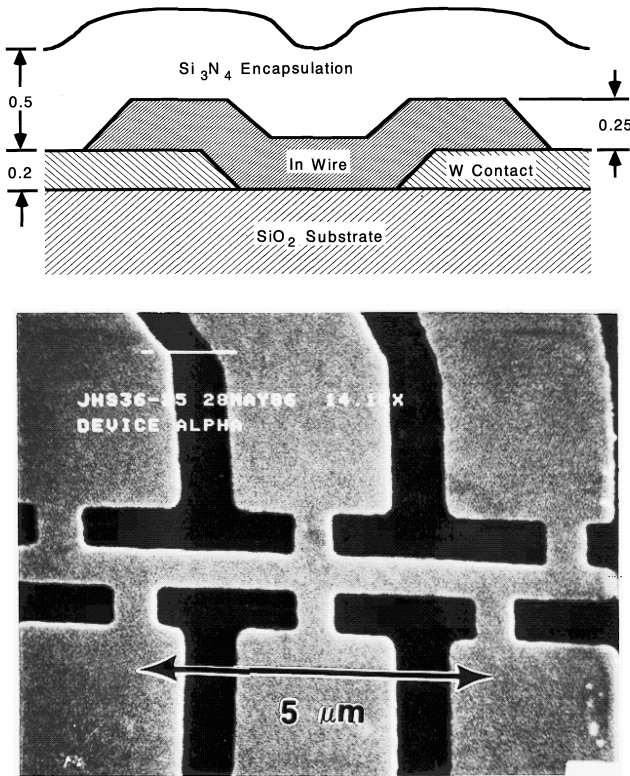


FIG. 1. (a) Cross sectional view of the encapsulated sample. Distances along the substrate are not drawn to scale. (b) Scanning electron micrograph of an unencapsulated, six-probe indium conductor.

For melting experiments it was necessary to encapsulate the indium with an insulator. This was accomplished by reactively sputtering a 300-500 nm layer of  $\text{Si}_3\text{N}_4$  over much of the chip leaving uncovered portions of the tungsten leads for wire-bonding. The chips were then mounted onto ceramic dual inline packages with conducting paint. Electrical connection to the devices was accomplished by ultrasonically bonding aluminum wires between the package and the tungsten contact leads.

Melting experiments were performed with the sample mounted in a vacuum can containing an optical window through which the sample could be viewed. The ceramic package was heat-sunk to a large copper block, thermally isolated from the rest of the can. Heat was supplied by a 50 watt heater mounted in the base of the block. Temperature was monitored with two chromel-alumel thermocouples inserted into holes drilled in the copper block, one just below the sample and the other at the heater. The temperature of the two thermocouples always agreed within the accuracy of the thermometry,  $\pm 1^\circ\text{C}$ . The copper block had a heat capacity ( $C$ ) of  $700 \text{ J/}^\circ\text{C}$  and a conductance ( $g$ ) to the room-temperature heat bath of  $60 \text{ mW/}^\circ\text{C}$ . No active temperature control was used so that near the melting transition noise measurements were limited to frequencies well above the inverse of the thermal relaxation time,  $C/g \approx 10^4 \text{ s}$ .

Resistance and resistance fluctuation measurements were made with the sample as part of an AC Wheatstone bridge (see Figure 2). The bridge error signal  $v_2(t) - v_1(t)$  was amplified and demodulated with a lock-in amplifier. The power spectral density  $S_V(f)$  of the lock-in output was measured using a fast fourier transform spectrum analyzer. Measurements of  $S_V(f)$  for different bias currents were combined to obtain the power spectral density  $S_r^-(f)$  of fluctuations in the difference between the resistances of the two halves of the sample,  $r_2 - r_1$ . It is important to note that the bridge error signal is insensitive to spatially correlated resistance fluctuations such as those due to sample temperature drifts. In the absence of spatial correlation,  $S_r^-(f)$  is the same as  $S_r(f)$ , where  $r \equiv r_1 + r_2$ . In all cases the excess noise spectra were proportional to the square of the rms-current; contact noise was determined to be insignificant. A detailed description of the measurement technique may be found elsewhere [13].

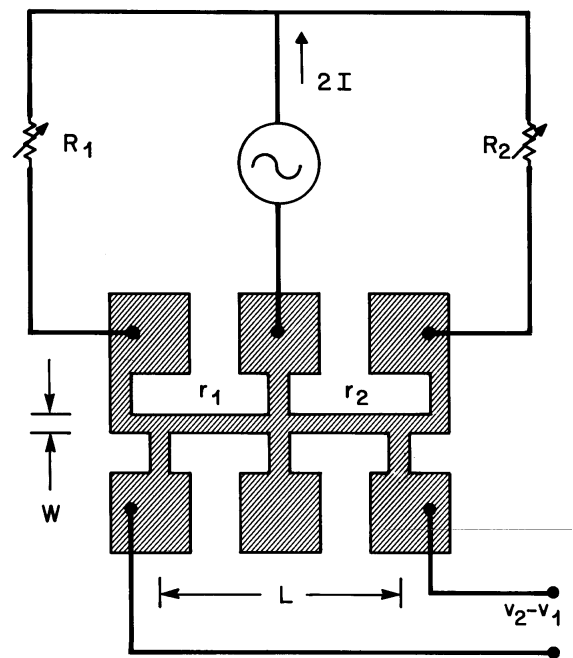
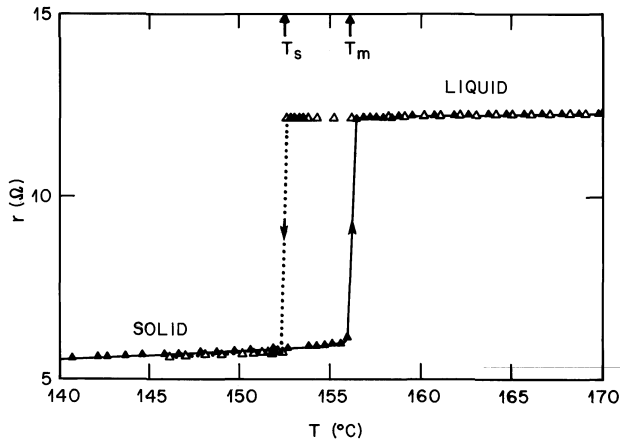


FIG. 2. Schematic diagram of the noise measurement circuit.

### III. Results

The resistance of several thick (250 nm) and thin (100 nm) samples were measured for temperatures  $20^\circ\text{C}$  to  $170^\circ\text{C}$ . The temperature dependence of the resistance near the melting transition of a thick encapsulated sample is plotted in Figure 3. Note that these data are not from the first melting cycle. The curves were obtained by combining  $r(t)$  data with  $T(t)$  data with interpolation in-between  $1^\circ\text{C}$  temperature increments (here  $t$  is time). The heating curve (solid symbols) and the cooling curve (open

symbols) exhibit hysteresis near the melting transition. Upon heating, the resistance of the solid indium film increases linearly with  $T$  due to phonon scattering.<sup>1</sup> As  $T$  approaches  $T_m = (156 \pm 1)^\circ\text{C}$  from below  $r(T)$  shows noticeable deviations from linearity then nearly doubles as the indium melts. The resistance of the liquid continues to increase with  $T$ , but at a slower rate than it did in the solid. Upon cooling, the resistance of the liquid retraces the heating curve down to  $T_m$ . The liquid super-cools, however, solidifying at  $T_s = (152 \pm 1)^\circ\text{C}$ . The resistance of the re-solidified indium falls near, but not exactly on the heating curve of the solid. Note that  $r(T)$  shows no precursor to solidifying as it does near melting.



**FIG. 3.** Temperature dependence of the resistance through the solid/liquid phase transition. The solid triangles were measured upon heating while the open triangles were measured upon cooling. The solid and dashed curves are guides to the eye. Absolute temperature is uncertain to  $\sim 1^\circ\text{C}$  while relative temperature is determined by interpolating time-temperature data. The melting temperature  $T_m$  and solidification temperature  $T_s$  are interpolated between the high and low resistance values.

All encapsulated samples exhibited  $r(T)$  similar to Figure 3. Unencapsulated samples had similar  $r(T)$  below  $T_m$ , but their resistances became infinite near  $T_m$  as the indium was observed to "ball up" and form discontinuous islands. The onset of a similar, but incomplete effect was observed to occur in the large indium probe regions of encapsulated samples the first time they were heated to  $T_m$ . Figure 4 is an optical micrograph of a sample after it has melted and resolidified. Note how the indium in the wide regions, especially over the tungsten contacts, has started to coalesce. This occurs because the  $0.5 \mu\text{m}$  thick  $\text{Si}_3\text{N}_4$  cap layer is not sufficiently rigid to hold back the 3% volume expansion of the indium upon melting in the larger regions. As a result, small indium structures are at a higher pressure, and accordingly, melt at a lower temperature than do large regions. The curvature in  $r(T)$  near melting is due to a nonuniform melting temperature in the indium probes. This has been verified by

<sup>1</sup> We have not looked for contributions to the resistance due to vacancy scattering.

comparing two-probe and four-probe resistance measurements.

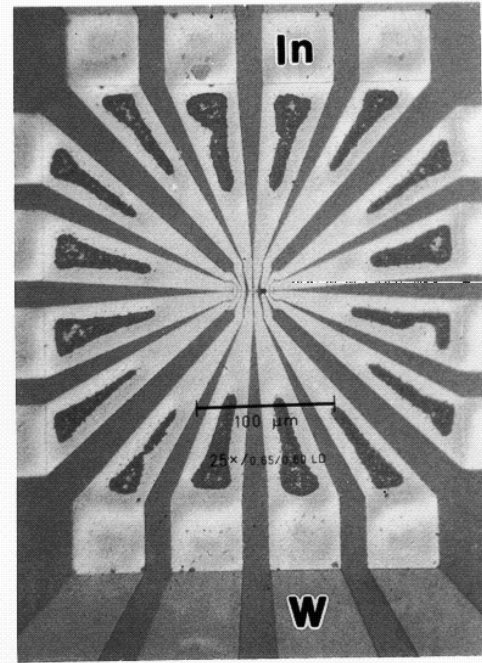


**FIG. 4.** Optical micrograph of an encapsulated sample after melting showing the effect of surface tension in the large indium probes.

Excess noise measurements for frequencies  $100 \text{ mHz} \leq f \leq 256 \text{ Hz}$  were performed on a total of four samples: a thin unencapsulated sample, a thick unencapsulated sample, a thin encapsulated sample, and a thick encapsulated sample (the sample of Figure 3). In all cases the excess noise was due to resistance fluctuations. Excess noise spectra of the unencapsulated samples were only measured at room temperature where they agreed with measurements from the corresponding encapsulated samples. The excess noise of the encapsulated samples were measured between  $20^\circ\text{C}$  and  $160^\circ\text{C}$ . Above  $150^\circ\text{C}$  the power spectra  $S_r^-(f)$  of the resistance fluctuations were "1/f-like;" that is,  $S_r^-(f) \propto f^{-\alpha}$  with the exponent  $\alpha = 1.20 \pm 0.05$ .<sup>2</sup>

Two types of noise measurements were made: 1) a "full" set of measurements at fixed temperature, and 2) a "short" set of measurements with the temperature slowly varying with time. The full set involved taking repeated measurements of the power spectrum for various bandwidths, bias currents, and checking for contact noise.

<sup>2</sup> At lower temperatures the excess noise of the thick sample deviated from a simple power law, exhibiting a single, broad peak in  $f S_r^-(f)$ . The peak occurred at 10 Hz at room temperature, shifted to higher frequency with increasing temperature, and disappeared from the observation bandwidth above  $148^\circ\text{C}$ . The excess noise of the thin sample did not deviate significantly from a power law at any temperature.

These measurements required about two hours, during which time the room (and sample) temperature drifted as much as 2 °C. It was not possible to make a full set of measurements very close to the melting transition. The short set consisted of just a few measurements of the power spectrum in a 1 Hz to 256 Hz bandwidth for a fixed bias current while the sample was heated or cooled at a rate on the order of 0.1 °C/minute. The short measurements required about 30 seconds.

The frequency exponent  $\alpha$  did not depend on temperature so that the temperature dependence of the noise is conveniently represented by the band-limited noise power, or noise level

$$\langle \delta r^2 \rangle \equiv \int_{1\text{Hz}}^{256\text{Hz}} S_r^-(f) df \quad (1)$$

The temperature dependence of  $\langle \delta r^2 \rangle$  for the thick encapsulated sample is plotted in Figure 5. The quantity plotted,  $N_a \langle \delta r^2 \rangle$ , is obtained by multiplying by the number of atoms in the conductor,  $N_a \approx 3 \times 10^{10}$  atoms. These data are not taken from the first melting cycle.<sup>3</sup> The solid symbols are measurements of  $\langle \delta r^2 \rangle$  upon heating. The four points with error bars represent a full set of measurements at fixed temperature while the rest of the points represent short measurements during heating. The noise level was nearly temperature independent in the solid, increased dramatically just prior to melting, and dropped by about an order of magnitude in the liquid. The joule heating and non-uniform melting of the indium probes made the bridge circuit very unstable near  $T_m$  during heating. Evidence suggests that noise increase near  $T_m$  is associated with fluctuations in the resistance of the indium contact leads. The open symbols in Figure 5 represent short data measurements with the sample cooling. The noise level of the liquid did not change with decreasing temperature until reaching  $T_s$ , whereupon the sample abruptly solidified and  $\langle \delta r^2 \rangle$  increased by nearly an order of magnitude.

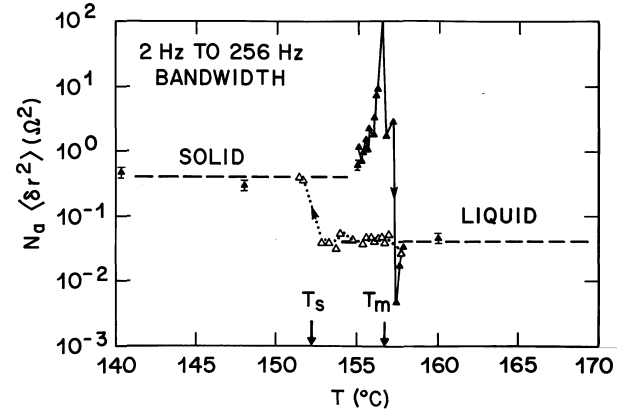


**FIG. 5.** Temperature dependence of the band-limited noise power of the resistance fluctuations through the solid/liquid phase transition,  $\langle \delta r^2 \rangle \equiv \int_{1\text{Hz}}^{256\text{Hz}} S_r^-(f) df$ . Similar to Figure 3, the solid triangles are measured upon heating while the open triangles are measured upon cooling. The four solid triangles with error bars at  $T = 140, 148, 155,$  and  $160^\circ\text{C}$  were measured at fixed temperature, varying bias and ballast resistance. The other data were measured with fixed current bias while the temperature changed steadily with time. The peak in the heating curve just prior to melting is thought to be due to contact noise.

The dashed lines in Figure 5 represent the noise level on either side of the solid/liquid phase transition. We believe that the structure in  $\langle \delta r^2 \rangle$  near  $T_m$ , during heating, is associated with the non-uniform melting of the probes (contact noise). Similar structure could well be present in the noise of the narrow indium conductor, but the absence of a "full" set of noise measurements near the transition makes it impossible for us to determine this.

Since the structure is present only during heating and not cooling, we are convinced that it is associated with the same non-uniform melting of the large contact regions that gives rise to the curvature in  $r(T)$  during heating.

#### IV. Discussion

The order of magnitude decrease in  $\langle \delta r^2 \rangle$  upon melting is consistent with the hypothesis that the dominant  $1/f$  noise is associated with slow defect processes present only in the solid. Still, the residual excess noise of the liquid displays a  $1/f$  spectrum demonstrating once again that the magnitude and mechanism for  $1/f$  noise are not universal. Since  $r$  doubles upon melting, the frequently quoted relative noise parameter,  $C_H = \left\{ f N_A S_r^-(f) / r^2 \right\}_{f=1\text{Hz}} \propto \langle \delta r^2 \rangle / r^2$ , is a factor of 40 - 10 lower for the liquid than for the solid. In contrast, Kedzia and Vandamme [9] found no change in  $C_H$  upon melting gallium point contacts. These new results support the arguments of Black et al. [10] against such point contact experiments.

There appear to be two noise mechanisms, the first being dominant in the solid and absent in the liquid, and the second, much smaller mechanism, being dominant in

<sup>3</sup> Very little data is available for the first melting cycle. What data there is suggests that not much different occurred than for subsequent cycles (with a factor of two uncertainty).

the liquid. It is possible that the second mechanism is also present in the solid; it could be associated with the indium/substrate or indium/Si<sub>3</sub>N<sub>4</sub> surfaces. The noise level  $N_a \langle \delta r^2 \rangle$  may be used to calculate  $C_H$  and  $r_*^2 \equiv \left\{ f N_A S_r(f) \right\}_{f=1\text{Hz}} = r^2 C_H q$  for comparison with the 1/f noise of other metallic films [3]. (Here,  $S_\rho(f)$  is the power spectral density of fluctuations in the specimen resistivity.) For the liquid this gives  $C_H \approx 5 \times 10^{-5}$  and  $r_*^2 \approx 0.06 (\mu\Omega\text{cm})^2$  respectively, comparable to the lowest 1/f noise levels reported for metals [3]. For the rest of the paper we discuss only the dominant noise mechanism.

Our results suggest that the dominant 1/f noise of the solid cannot be associated with phonon scattering. The argument is simple. The doubling of the resistance upon melting is due to the loss of long-range order and is associated with increased phonon scattering. Were the resistance fluctuations associated with this same scattering mechanism,  $\langle \delta r^2 \rangle$  would also increase upon melting [9]; it does not. Instead,  $\langle \delta r^2 \rangle$  decreases upon melting. Therefore the noise is not associated in any simple way with phonon scattering.

We also argue that the dominant noise is not likely to be associated with impurity scattering. The argument is similar to that above. Impurity concentrations in the solid and liquid should be the same, though their spatial distribution would differ. Therefore, we would not expect much change in the *total noise power* upon melting were the noise simply related to impurity scattering. We observe upon melting, however, an order of magnitude decrease in the band-limited noise power  $\langle \delta r^2 \rangle$ . Dutta et.al. have shown that the noise power in any bandwidth can change with temperature quite independently of the total noise power, due to thermally activated rates [1,13]. Such processes, however, will exhibit related changes with temperature of their frequency dependence, i.e., the frequency exponent  $\alpha = \alpha(T)$ . We do not observe any such change in the slope  $\alpha$ . Therefore, we assume that  $\langle \delta r^2 \rangle$  reflects the temperature dependence of the total noise power.<sup>4</sup>

The disappearance of the dominant noise source upon melting has significant implications as to the kinds of defects that may be involved. Impurities alone cannot be the source since the impurity concentration in the liquid and solid are probably the same. However, the

interaction of impurities (or point defects) with other defects could account for the dominant noise of the solid. The possible defect-defect interactions range from local two-level systems [5] to longer range diffusion with extended defects acting as sources/sinks of point defects or impurities [3,8].

Grain boundaries, thought to be associated with the 1/f noise of aluminum films [5] could account for the decrease in noise upon melting but not for other aspects of the noise. For instance, the room temperature excess noise of the re-solidified film is not much different from that of the as-deposited film. The crystallite size, on the other hand, is believed to be initially very small and to grow during the initial heating cycle. The re-solidified conductor is likely to contain few grain boundaries if any. Subsequent melting cycles are not likely to yield further changes in the film microstructure. Data from the first melting cycle are limited, but suggest that  $\langle \delta r^2 \rangle$  did not change much with annealing cycles.

While questions remain, our result demonstrates the importance of the lattice as has been found for other systems. Jackel et al. [14] found that the trapping/detrapping rates of electrons in narrow silicon MOSFETs varied with the lattice temperature, not the electron temperature. Rogers et al. [15] have suggested that conductance fluctuations in tunnel junctions at low temperatures are related to configurational tunneling of ions.

## V. Conclusions

In conclusion, we have fabricated thin continuous indium film conductors on an insulating substrate in submicron geometries suitable for four-probe resistance and noise measurements above their melting temperature. The power spectrum of the low frequency excess noise of these conductors has been measured for temperatures surrounding their liquid/solid phase transition. We found that the excess noise had a 1/f-spectrum, was attributable to resistance fluctuations, and that the relative noise power was about 40 times lower for the liquid than for the solid. The result indicates that the lattice plays an important role in generating 1/f noise, and is consistent with several defect models for 1/f noise. These encapsulated indium samples represent a rich system for studying the effects of defects on noise and resistance of thin metal films.

## Acknowledgments

The authors would like to thank P. Mankiewich and R. Howard for many suggestions during sample fabrication. Thanks also go to L. Jackel, J. Mantese, and W. Skocpol for useful discussions.

<sup>4</sup> It is important to keep in mind that we are measuring the spectrum of fluctuations in the difference  $r_2 - r_1$ , not  $r_2 + r_1$ . All previous measurements of 1/f noise have failed to find any spatial correlation. Without spatial correlation, the two spectra are the same. It is possible, however, for rapid diffusion to result in spatial correlation for resistivity fluctuations.

## References

1. Useful reviews are P. Dutta and P. M. Horn, *Rev. Mod. Phys.* **53**, 497 (1981); and M. B. Weissman, *Rev. Mod. Phys.* **60**, 537 (1988).
2. D. M. Fleetwood and N. Giordano, *Phys. Rev. B* **31**, 1157 (1985).
3. John H. Scofield, Joseph V. Mantese, and Watt W. Webb, *Phys. Rev. B* **32**, 736 (1985).
4. Jonathoan Pelz and John Clarke, *Phys. Rev. Lett.* **55**, 738 (1985).
5. R. H. Koch, J. R. Lloyd, and J. Cronin, *Phys. Rev. Lett.* **55**, 2487 (1985).
6. Sh. M. Kogan and K. E. Nagaev, *Sov. Phys. Solid State* **24**, 1921 (1982).
7. R. D. Black, P. J. Restle, and M. B. Weissman, *Phys. Rev. Lett.* **51**, 1476 (1983).
8. John H. Scofield and Watt W. Webb, *Phys. Rev. Lett.* **54**, 353 (1985).
9. Jozef Kedzia and L. K. J. Vandamme, *Phys. Lett.* **66A**, 313 (1978).
10. R. D. Black, P. J. Restle, and M. B. Weissman, *Phys. Rev. B* **28**, 1935 (1983).
11. John H. Scofield, Roger W. Epworth, and D. M. Tennant, in *Science and Materials Research Society Symposia Proceedings, Vol. 76: Science and Technology of Microfabrication* (Materials Research Society, Pittsburgh, 1987). pp. 85-89.
12. R. Y. Chiao, M. J. Feldman, H. Ohta, and P. T. Parrish, *Rev. de Phys. Appl.* **9**, 183 (1974). 13. John H. Scofield, *Rev. Sci. Instrum.* **58**, 985 (1987).
13. P. Dutta, P. Dimon, and P.M. Horn, *Phys. Rev. Lett.* **43**, 646 (1979).
14. L. D. Jackel, W. J. Skocpol, R. E. Howard, L. A. Fetter, R. W. Epworth, and D. M. Tennant, in *Proceedings of the 17th International Conference on the Physics of Semiconductors*, edited by J. D. Chadi and W. A. Harrison (Springer-Verlag, New York, 1985), p. 221.
15. C. T. Rogers and R. A. Buhrman, *Phys. Rev. Lett.* **55**, 859 (1985).